DRAFT VERSION OCTOBER 18, 2016
Preprint typeset using LaTeX style emulateapj v. 5/2/11

arXiv:1610.01373v2 [astro-ph.HE] 17 Oct 2016

COMPRESSIBLE RELATIVISTIC MAGNETOHYDRODYNAMIC TURBULENCE IN MAGNETICALLY-DOMINATED PLASMAS AND IMPLICATIONS FOR A STRONG-COUPLING REGIME

MAKOTO TAKAMOTO
Department of Earth and Planetary Science, The University of Tokyo, Hongo, Bunkyo-ku, Tokyo, 113-0033, Japan

ALEXANDRE LAZARIAN
Department of Astronomy, University of Wisconsin, 475 North Charter Street, Madison, WI 53706, USA
Draft version October 18, 2016

ABSTRACT

In this Letter, we report compressible mode effects on relativistic magnetohydrodynamic (RMHD) turbulence in Poynting-dominated plasmas using 3-dimensional numerical simulations. We decomposed fluctuations in the turbulence into 3 MHD modes (fast, slow, and Alfvén) following the procedure mode decomposition in (Cho & Lazarian 2002), and analyzed their energy spectra and structure functions separately. We also analyzed the ratio of compressible mode to Alfvén mode energy with respect to its Mach number. We found the ratio of compressible mode increases not only with the Alfvén Mach number but with the background magnetization, which indicates a strong coupling between the fast and Alfvén modes and appearance of a new regime of RMHD turbulence in Poynting-dominated plasmas where the fast and Alfvén modes strongly couples and cannot be separated, different from the non-relativistic MHD case. This finding will affect particle acceleration efficiency obtained by assuming Alfvénic critical balance turbulence, and will change the resulting photon spectra by non-thermal electrons.

Subject headings: magnetic fields, magnetohydrodynamics (MHD), relativistic processes, plasmas, turbulence

1. INTRODUCTION

Turbulence is ubiquitous in many plasma phenomena. Over the past few decades, a considerable number of studies have been conducted on the properties of non-relativistic magnetohydrodynamic (MHD) turbulence, and they have revealed many interesting and essential properties, for example, the critical-balance condition of strong turbulence (Goldreich & Sridhar 1995; Beresnyak & Lazarian 2010; Beresnyak 2014), the existence of weak turbulence (Iroshnikov 1964; Kraichnan 1965; Galtier et al. 2000; Meyrand et al. 2016), and mode coupling between Alfvénic and compressible modes (Cho & Lazarian 2002, 2003). The concern with relativistic turbulence has recently been growing because of the development of high-power laser plasma devices and observation devices for high-energy astrophysical phenomena. In particular, the observation of high energy astrophysical phenomena, such as gamma-ray bursts and flares of relativistic jets, indicates that there will be strong turbulence that is necessary for acceleration of electrons emitting non-thermal photons observed from those phenomena (Hayashida et al. 2012; Asano & Hayashida 2015). Recent theoretical studies of those phenomena indicate that the background plasma of those phenomena is Poynting-energy dominated (Kennel & Coroniti 1984a,b; Kino et al. 2015) in which the relativistic magnetization parameter, $\sigma \equiv B_0^2/4\pi\rho hc^2\gamma^2$, is larger than unity where B_0 is the background magnetic field, ρ is the rest mass density, h is the specific enthalpy, c is the velocity of light, and γ is the Lorentz factor [1]. Although there are several works investigating turbulence in relativistic MHD plasma (Inoue et al. 2011; Zrake & MacFadyen 2012, 2013; Radice & Rezzolla 2013; Takamoto et al. 2015) and force-free plasma (Thompson & Blaes 1998; Cho 2005; Cho & Lazarian 2014), many properties of the relativistic MHD turbulence and the dependence on the background σ-parameter are still unclear, in particular, in the case of Poynting-dominated RMHD turbulence.

In this Letter, we report our findings on RMHD turbulence, in particular, the properties of each MHD characteristic mode in low-β plasma but covering low-σ to high-σ plasma for the first time. We performed a series of numerical relativistic MHD simulations of turbulence, and analyzed the spectral properties of each mode, their structure function, and eddy-scale in terms of local mean field. We also discuss a possibility of a strong coupling between the fast and Alfvén modes and appearance of a new regime of RMHD turbulence in Poynting-dominated plasmas where the fast and Alfvén modes strongly couples and cannot be separated, different from the non-relativistic MHD case.

2. NUMERICAL SETUP

The plasma is modeled by the ideal RMHD approximation with the TM equation of state (Mignone et al. 2005) that allows us to simulate the relativistic perfect gas equation of state (Synge 1957) with less than 4 % error. The equations are updated by the relativistic HLLD method (Mignone et al. 2009) in a conservative fashion using the constrained transport algorithm (Evans & Hawley 1988; Gardiner & Stone 2005). The initial background plasma is assumed to be uniform with a uniform magnetic field $\mathbf{B}_0$, density ρ_0, and temperature $k_B T = 0.1mc^2$ where k_B is the Boltzmann constant, T is the temperature, m is the particle mass. We injected an isotropic turbulent mode component at the initial time-step, so-called *decaying*

mtakamoto@eps.s.u-tokyo.ac.jp
alazarian@facstaff.wisc.edu

[1] Note that the σ-parameter is originally defined as a ratio between Poynting-flux to particle energy flux. The form introduced in this Letter is a reduced one assuming MHD approximation $\mathbf{E} = \mathbf{v}/c \times \mathbf{B}$ that can be used in a static background flow. It also becomes the square of relativistic 4-Alfvén velocity in the fluid comoving frame, and is popular in high energy astrophysics community.

turbulence. Similar to (Takamoto et al. 2015), we injected the turbulence at large scales, $l_{\rm inject} = L/2, L/3, L/4$, where L is the numerical box size, and the energy spectrum is assumed to be flat. Following (Cho & Lazarian 2002, 2003), the turbulence is injected only with an Alfvén mode velocity component that is obtained by the method explained in the next section. We consider a cubic numerical domain that is divided by uniform meshes whose size is typically $\Delta = L/512$ to obtain fast to Alfvén mode power ratio (Figure 1); we use higher resolutions, $\Delta = L/1024, L/2048$, to obtain the energy spectra and the structure functions provided in Figure 2 ($L/1024$ for $\sigma = 0.2, 1$ and $L/2048$ for $\sigma = 3$). The resolution is chosen as sufficient for resolving turbulent-eddies responsible for the mode exchange in our simulation [2].

3. MODE DECOMPOSITION OF RMHD TURBULENCE

Following (Cho & Lazarian 2002, 2003), we consider the displacement vectors of slow and fast modes. Since there is no average velocity in the background flow, the displacement vectors reduce to:

$$\hat{\xi}_{\rm slow} \propto k_{||}\hat{\mathbf{k}}_{||} + \left[\frac{u_{\rm slow}^2}{c_{\rm s}^2}\left(\frac{k}{k_{||}}\right)^2 - 1\right]\left[\frac{k_{||}}{k_\perp}\right]^2 k_\perp \hat{\mathbf{k}}_\perp, \quad (1)$$

$$\hat{\xi}_{\rm fast} \propto \left[u_{\rm fast}^2 k^2(1+\sigma) - c_{\rm s}^2 k_\perp^2 - k^2\sigma\right]\left[\frac{1}{c_{\rm s}k_{||}}\right]^2 k_{||}\hat{\mathbf{k}}_{||} + k_\perp\hat{\mathbf{k}}_\perp, \quad (2)$$

where c_s is the relativistic sound velocity, k is the absolute value of the wave vector $\mathbf{k}$, and $u_{\rm fast/slow}$ are the characteristic velocities of fast and slow modes (Anile 1990). $k_{||}, k_\perp$ are taken as the parallel and perpendicular to the background magnetic field direction ($\mathbf{B}_0$). Note that Equations (1) and (2) reduce to the Equations (1) and (2) of (Cho & Lazarian 2002) if we take the non-relativistic limit and set $c_{\rm s} = 0.1$ and $c_{\rm A} = 1$ where c_A is the Alfvén velocity. Equations (1) and (2) allow us to obtain fast and slow mode velocity components by projecting the velocity field on the displacement vectors $\hat{\xi}_{\rm fast/slow}$. Similar to the non-relativistic case, the displacement vector of the Alfvén mode velocity component is given as: $\hat{\xi}_{\rm A} = \hat{\mathbf{k}}_{||} \times \hat{\mathbf{k}}_\perp$ (Maron & Goldreich 2001). In the following, we write the velocity projection onto $\xi_{\rm \{A,fast,slow\}}$ as $\delta v_{\rm \{A,f,s\}}$. Since the form of the linearized mass conservation law and induction equation are the same as the non-relativistic ones, the Fourier components of density and magnetic field can be obtained by exactly the same procedure in the non-relativistic case given in (Cho & Lazarian 2002, 2003). We should stress that, for turbulence, the mode decomposition is valid in a statistical sense as it discussed in (Cho & Lazarian 2002). Moreover, the meaning of the decomposition is different for the case of weak and strong coupling of modes. When the transfer of energy between the modes is weak as it is the case of non-relativistic turbulence, the mode decomposition reveals the distinct cascades among Alfvén, fast, and slow mode (Cho & Lazarian 2002). In the case of relativistic turbulence, as the coupling increases the decomposition reveals the transfer of energy between the cascades.

When we calculated the kinetic power, the energy spectrum, and the 2nd-order structure functions of each mode, we projected the Fourier component of velocity onto the displacement vectors, and performed inverse Fourier transformation of each decomposed component in real-space.

[2] "*ideal*" RMHD means that no explicit dissipation processes are included, such as the viscosity, thermal conductivity, and resistivity. However, the explicit differential scheme we employed here always include the numerical grid-scale dissipation, which allows the dissipation at the smallest-eddy and direct cascade of energy into smaller scale.

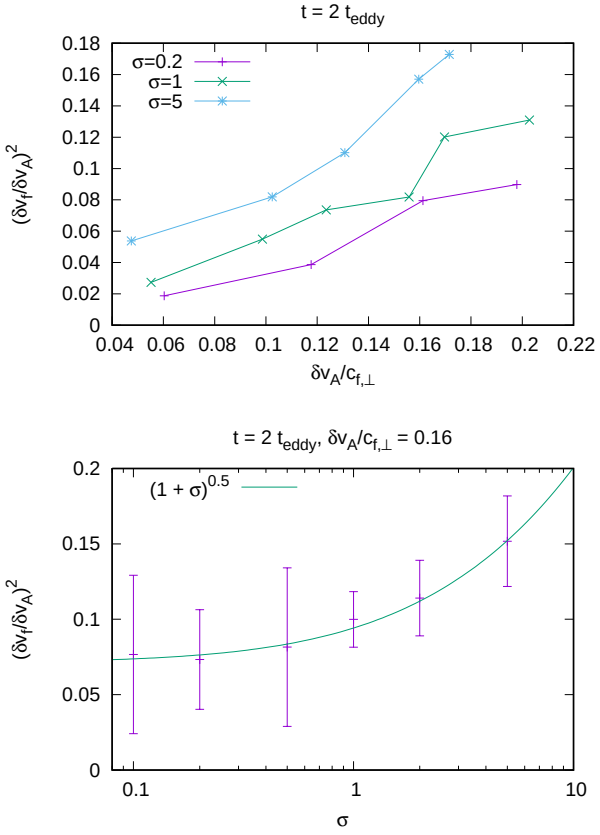

FIG. 1.— Left: The ratio of fast to Alfvén mode velocity power in terms of the non-relativistic fast Mach number of the Alfvén mode component using 3-velocity. This indicates that the compressible mode becomes more important with increasing σ-parameter. Right: The ratio of fast to Alfvén mode velocity power in terms of the background σ parameter at $t = 2t_{\rm eddy}$ and $\delta v_{\rm A}/c_{\rm f,\perp} = 0.16$ whose values are obtained by fitting of the curves of each σ-value by linear curves. Note that the error bar results from the fitting of the curves. This shows that the ratio is proportional with $\sqrt{1+\sigma}$ when $\sigma > 1$.

4. RESULTS

The left panel of Figure 1 is the ratio of fast to Alfvén mode velocity power at 2 eddy-turnover time in terms of the fast Mach number of the Alfvén component of velocity. Each point corresponds to a simulation result with an injection velocity. Note that the fast velocity $c_{\rm f,\perp}$ in the horizontal axis is taken as that in the perpendicular direction to the background magnetic field. The curves in the panel show that the fast mode power increases nearly linearly with the fast Mach number as reported in the non-relativistic case (Cho & Lazarian 2002, 2003). In addition, it also shows that the fast component increases with σ-value. The right panel of Figure 1 is the ratio of fast to Alfvén mode velocity power in terms of the background σ value at $t = 2t_{\rm eddy}$ and $\delta v_{\rm A}/c_{\rm f,\perp} = 0.16$. It shows the ratio is nearly independent of the σ-parameter when $\sigma < 1$ whose value is around 0.08. Note that this indicates the Alfvén to fast energy conversion is not more than 8% in the low-σ plasma, which is consistent with the result obtained by (Cho & Lazarian 2002). On the other hand, it increases approximately by $(1+\sigma)^{1/2}$ when $\sigma > 1$, which is basically consistent with our previous result of the driven turbulence (Takamoto et al. 2015). This indicates that the ratio

can be written as:

$$(\delta v_{\rm f})^2/(\delta v_{\rm A})^2 \propto (\delta v_{\rm A})/c_{\rm fast,\perp} \qquad (\text{when } \sigma \ll 1), \tag{3}$$

$$\propto (1+\sigma)^{1/2}(\delta v_{\rm A})/c_{\rm fast,\perp} \qquad (\text{when } \sigma \gtrsim 1). \tag{4}$$

Note that this is a relativistic extension of the Equation (6) in (Cho & Lazarian 2002). This indicates that the non-linearity of the Alfvén mode becomes strong enough to convert its energy into compressible mode at this value of fast Mach number as the electromagnetic field becomes relativistically strong. Qualitatively, this can be explained by the electric field that should be taken into account in the relativistic MHD equations because of the relativistic velocity: $|\mathbf{E}| = |-(\mathbf{v}/c)\times\mathbf{B}| \sim |\mathbf{B}|$. If we use the quasi-linear theory, that is, take into account the 2nd-order terms in equations assuming 1st-order Alfvén mode perturbation, the force term in the equation of motion of RMHD can be written as:

$$F_{\rm x} \equiv -\nabla_x \left[\frac{B_0^2}{2}\left(1+\frac{c_{\rm A}^2}{c^2}\right)\left(\frac{\delta v_{\rm A}}{c_{\rm A}}\right)^2\right], \tag{5}$$

$$F_{\rm y} \equiv -\nabla_y \left[\frac{B_0^2}{2}\left(1-\frac{c_{\rm A}^2}{c^2}\right)\left(\frac{\delta v_{\rm A}}{c_{\rm A}}\right)^2\right], \tag{6}$$

$$F_{\rm z} \equiv -B_0\nabla_x \delta B_{\rm A}, \tag{7}$$

where we set the background magnetic field as $\mathbf{B}_0 = B_0\mathbf{e}_x$ and the Alfvén mode direction in z-direction. The z-component drives the usual Alfvén mode. Interestingly, the anisotropic nature of the electric field gives the weaker force in the y-direction and the stronger force in x-direction, or the parallel direction of the background magnetic field. In the Poynting-dominated regime, $c_{\rm A} \sim c$, the force is only in the direction parallel to the magnetic field direction, and we consider this is the origin of increasing fast mode conversion. Note that this also indicates that the mode coupling between fast and Alfvén modes becomes stronger, which is not observed in non-relativistic MHD turbulence (Cho & Lazarian 2002). Rewriting Equation (4) as, $(\delta v_{\rm F}/\delta v_{\rm A})^2 \simeq \alpha\sqrt{1+\sigma}$, where $\alpha \equiv 0.4\delta v_{\rm A}/c_{\rm fast,\perp}$ whose coefficient 0.4 is obtained by the fitting data in Figure 1, the completely coupling of fast and Alfvén modes, $\delta v_{\rm F} \sim \delta v_{\rm A}$, occurs when $\sigma \sim 1/\alpha^2 - 1$; If we assume $\delta v_{\rm A}/c_{\rm fast,\perp} \sim 0.5$, the necessary σ value becomes around 24. In this regime, we can expect an appearance of a new RMHD turbulence regime where the critical balance is invalid due to the strong coupling to the fast mode. Concerning the slow mode conversion, we found that slow modes also show similar behavior to the fast mode as shown in Figure 1, but their kinetic energy is approximately 1.5 times larger than the fast mode case. We take this to be due to the fact that the considered turbulence is in the regime of sub-Alfvénic but super-slow turbulence. More detailed analysis will be reported in our forthcoming papers.

Importantly, the fast to Alfvén mode power ratio depends on a 3-fast Mach number, not the relativistic 4-fast Mach number. This means that in Poynting-dominated plasma the compressible mode turbulence becomes important even if the kinetic energy of the turbulence is much smaller than the background magnetic field energy, and this is very different from the non-relativistic case whose kinetic energy of turbulence should be comparable to the background magnetic field energy, $\rho v_{\rm turb}^2 \sim B^2$. This will be important for the electron and cosmic-ray acceleration by MHD turbulence (Fermi 1949, 1954) in high-energy astrophysical phenomena, such as GRBs and blazars (see e.g. (Asano & Hayashida 2015)) [3]

Alfvén Mode–The top-left panel of Figure 2 shows the kinetic energy spectrum of Alfvén mode in terms of the wave vector perpendicular to the background magnetic field. It indicates that the spectrum follows the Kolmogorov spectrum in its inertial region:

$$E^{\rm A}(k_\perp) \propto k_\perp^{-5/3}, \tag{8}$$

which is consistent with the critical balance predicted by (Goldreich & Sridhar 1995), meaning the energy-cascade time by Alfvén mode along the magnetic field is comparable to that by eddy-interaction perpendicular to the magnetic field, and the turbulent eddy becomes anisotropic [4]. Note that this is also consistent with the results by (Zrake & MacFadyen 2012, 2013; Radice & Rezzolla 2013) that performed not the mode decomposition but the Helmholtz decomposition of velocity, although the incompressible mode obtained by the Helmholtz decomposition is essentially different from the Alfvén mode. The bottom-left panel of Figure 2 shows the values of $r_{||}$ and $r_\perp$ with the same 2nd-order structure function for the velocity. The distance $r_{||}$ and $r_\perp$ is determined using the local magnetic field direction following (Cho & Vishniac 2000). Note that it is essential to measure $r_{||}$ and $r_\perp$ in terms of the local mean magnetic field because the critical balance proposed by (Goldreich & Sridhar 1995) is applicable only in the local system of reference, which was established by (Lazarian & Vishniac 1999; Cho & Vishniac 2000; Maron & Goldreich 2001; Cho et al. 2002). It shows that the eddy size scales as $k_{||} \propto k_\perp^{2/3}$ as predicted by (Goldreich & Sridhar 1995). Our simulation results indicate that the critical balance is still valid in high-σ regime which is consistent with works assuming the force-free approximation (Thompson & Blaes 1998; Cho 2005; Cho & Lazarian 2014) [5].

Fast Mode–The top-middle panel of Figure 2 shows the kinetic energy spectrum of fast mode in terms of the wave vector perpendicular to the background magnetic field. It indicates that the energy spectrum of their inertial region can be written as:

$$E^{\rm f}(k) \propto k^{-3/2} \qquad (\text{when } \sigma < 1), \tag{9}$$

$$\propto k^{-1.86} \qquad (\text{when } \sigma > 1). \tag{10}$$

The value of the spectrum index 1.86 is previously obtained by (Zrake & MacFadyen 2012, 2013) which did not perform mode decomposition but considered the compressible component (potential component) $\mathbf{u}_{\rm p} = \nabla\phi$ where ϕ is a scalar function. Note that our results indicates that the index becomes

[3] The enhancement of compressibility effects was mentioned in (Radice & Rezzolla 2013) in the relativistic temperature case, but in the paper we quantify this effects covering Poynting-energy dominated regime.

[4] Note that it is still very difficult to judge if the spectrum index is $-5/3$ or -1.5 due to the insufficient numerical resolution. The effects of the bottleneck (Beresnyak & Lazarian 2010; Beresnyak 2014; Beresnyak & Lazarian 2015) might also distort the measured spectra.

[5] Note that we observed only the *strong turbulence* regime, though we injected sub-Alfvénic turbulence that induces the *weak turbulence* in the large scale regime as first pointed out in (Lazarian & Vishniac 1999). We take this to indicate that the resolution in the direction perpendicular to the background magnetic field is not enough to observe the weak turbulence cascade. It may also be because the generation of compressible modes hinders the Alfvén mode energy in cascading in the perpendicular direction (pointed out by Sébastien Galtier). Recent findings of the weak turbulence regime in numerical simulations are reported by (Meyrand et al. 2016).

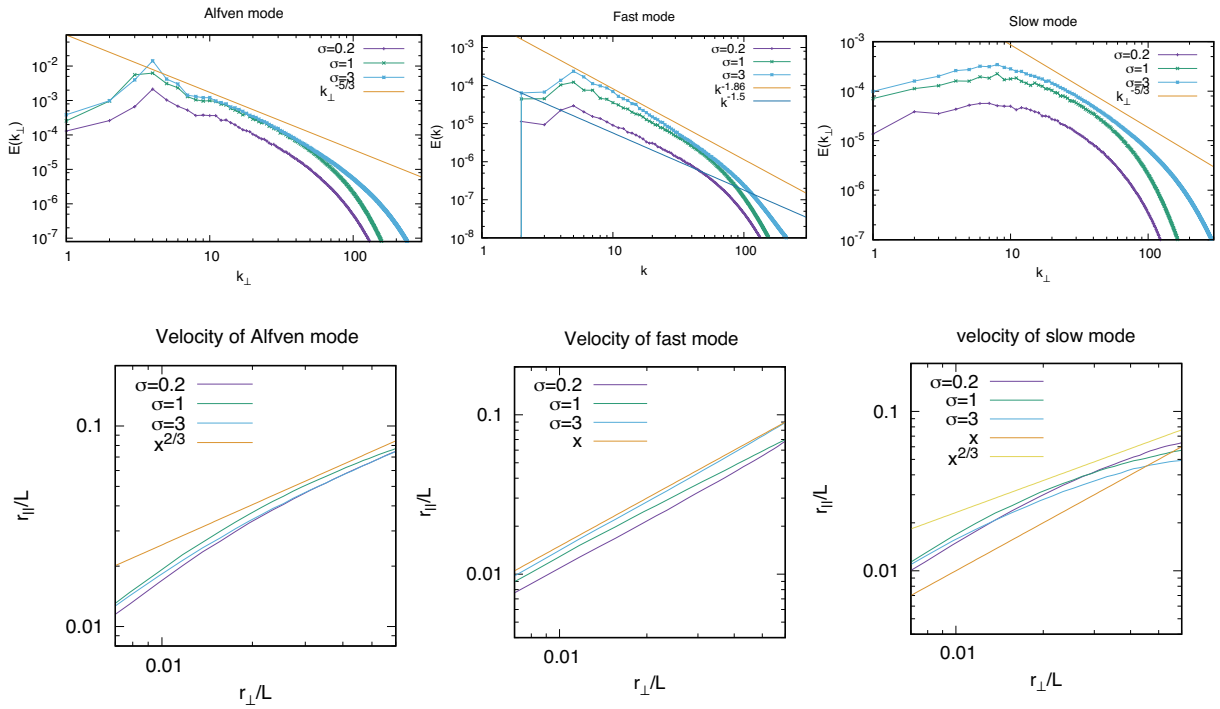

FIG. 2.— Top: Kinetic energy spectra of Alfvén, fast, and slow mode. Bottom: Eddy-scale of Alfvén, fast, and slow mode obtained by a 2nd-order velocity structure function. All the data are measured at 1 eddy-turnover time. The initial Alfvén mode turbulence is injected at $k/2\pi = 3/L$ with velocity dispersion $\delta v/c_{\rm A} = 0.6$ for $\sigma = 0.2, 1$ and $\delta v/c_{\rm A} = 0.5$ for $\sigma = 3$.

slightly larger than 1.86, and an increasing function of σ. The bottom-middle panel of Figure 2 shows the values of $r_{||}$ and $r_\perp$ of fast mode turbulent eddy. It indicates that the eddy is nearly isotropic, $r_{||} \propto r_\perp$ independent of its scale, similar to the non-relativistic case.

Slow Mode–The top-right panel of Figure 2 shows the kinetic energy spectrum of slow mode in terms of the wave vector perpendicular to the background magnetic field. The indicated energy spectrum indicates the non-power law behavior even as the resolution is increased from L/512 to L/2024. This may signify that the energy exchange between slow mode and Alfven becomes stronger than in the case of non-relativistic turbulence in (Cho & Lazarian 2002). The bottom-right panel of Figure 2 shows the values of $r_{||}$ and $r_\perp$ of the slow mode turbulent eddy. It indicates that the slow mode eddy size also follows the critical condition, similar to the Alfvén mode. We take these results to indicate that the slow mode, or the pseudo-Alfvén mode, do not cascade its energy for themselves as is known to occur in the non-relativistic case (Lithwick & Goldreich 2001; Cho & Lazarian 2002).

5. DISCUSSION AND CONCLUSION

In this Letter, we investigated the properties of each characteristic mode of the relativistic ideal MHD turbulence. The most important finding is that the ratio of fast to Alfvén mode velocity power increases not only with the fast Mach number of the Alfvén mode velocity, but with the background σ-parameter when $\sigma > 1$. This indicates that the mode coupling between fast and Alfvén modes becomes stronger in Poynting-dominated plasmas, which is not observed in non-relativistic MHD turbulence. This also suggests that a new turbulence regime will appear in a sufficiently high-σ plasma where Alfvén mode and fast mode completely couples, and the critical-balance cannot be applied. We also investigated the behavior of the energy spectra and eddy shapes. Although Alfvén and slow modes show a similar behavior to their non-relativistic cases, the energy spectrum of fast mode shows a different behavior whose spectrum index increases from $3/2$ to more than 1.86 with σ-parameter. Our finding will advance our understanding of high-energy astrophysical phenomena, for example, the acceleration of electrons resulting in the observed non-thermal photon energy spectrum (Fermi 1949, 1954; Petrosian & Liu 2004; Lazarian & Yan 2014), enhancement of magnetic reconnection responsible for relativistic jet acceleration (Takamoto et al. 2015; Singh et al. 2016), and cosmic-ray diffusion in turbulent media (Lazarian & Yan 2014). It also indicates that the compressible turbulence will be involved in many high-energy astrophysical objects with Poynting-dominated plasma, such as the pulsar wind nebulae, relativistic jets, and GRBs.

We would like to thank Sébastien Galtier, Supratik Banerjee, and Nobumitsu Yokoi for many fruitful comments and discussions. Numerical computations were carried out on the Cray XC30 at Center for Computational Astrophysics, CfCA, of National Astronomical Observatory of Japan. Calculations were also carried out on SR16000 at YITP in Kyoto University. This work is supported in part by the Postdoctoral Fellowships by the Japan Society for the Promotion of Science No. 201506571 (M. T.). AL is supported by NSF AST 1212096, NASA grant X5166204101.

REFERENCES

Anile, A. M. 1990, Relativistic Fluids and Magneto-fluids, 348
Asano, K., & Hayashida, M. 2015, ApJL, 808, L18
Beresnyak, A. 2014, ApJL, 784, L20
Beresnyak, A., & Lazarian, A. 2010, ApJL, 722, L110

Beresnyak, A., & Lazarian, A. 2015, in Astrophysics and Space Science Library, Vol. 407, Magnetic Fields in Diffuse Media, ed. A. Lazarian, E. M. de Gouveia Dal Pino, & C. Melioli, 163
Cho, J. 2005, ApJ, 621, 324
Cho, J., & Lazarian, A. 2002, Physical Review Letters, 88, 245001
—. 2003, MNRAS, 345, 325
—. 2014, ApJ, 780, 30
Cho, J., Lazarian, A., & Vishniac, E. T. 2002, ApJ, 564, 291
Cho, J., & Vishniac, E. T. 2000, ApJ, 539, 273
Evans, C. R., & Hawley, J. F. 1988, ApJ, 332, 659
Fermi, E. 1949, Physical Review, 75, 1169
—. 1954, ApJ, 119, 1
Galtier, S., Nazarenko, S. V., Newell, A. C., & Pouquet, A. 2000, Journal of Plasma Physics, 63, 447
Gardiner, T. A., & Stone, J. M. 2005, Journal of Computational Physics, 205, 509
Goldreich, P., & Sridhar, S. 1995, ApJ, 438, 763
Hayashida, M., et al. 2012, ApJ, 754, 114
Inoue, T., Asano, K., & Ioka, K. 2011, ApJ, 734, 77
Iroshnikov, P. S. 1964, Sov. Astron., 7, 566
Kennel, C. F., & Coroniti, F. V. 1984a, ApJ, 283, 694
—. 1984b, ApJ, 283, 710
Kino, M., Takahara, F., Hada, K., Akiyama, K., Nagai, H., & Sohn, B. W. 2015, ApJ, 803, 30
Kraichnan, R. H. 1965, Physics of Fluids, 8, 1385
Lazarian, A., & Vishniac, E. T. 1999, ApJ, 517, 700
Lazarian, A., & Yan, H. 2014, ApJ, 784, 38
Lithwick, Y., & Goldreich, P. 2001, ApJ, 562, 279
Maron, J., & Goldreich, P. 2001, ApJ, 554, 1175
Meyrand, R., Galtier, S., & Kiyani, K. H. 2016, Physical Review Letters, 116, 105002
Mignone, A., Plewa, T., & Bodo, G. 2005, ApJS, 160, 199
Mignone, A., Ugliano, M., & Bodo, G. 2009, MNRAS, 393, 1141
Petrosian, V., & Liu, S. 2004, ApJ, 610, 550
Radice, D., & Rezzolla, L. 2013, ApJL, 766, L10
Singh, C. B., Mizuno, Y., & de Gouveia Dal Pino, E. M. 2016, ArXiv e-prints
Synge, J. L. 1957, The relativistic gas, Vol. 32 (North-Holland Amsterdam)
Takamoto, M., Inoue, T., & Lazarian, A. 2015, ApJ, 815, 16
Thompson, C., & Blaes, O. 1998, Phys. Rev. D, 57, 3219
Zrake, J., & MacFadyen, A. I. 2012, ApJ, 744, 32
—. 2013, ApJL, 763, L12